GEOPHYSICAL RESEARCH LETTERS, VOL. 25, NO.15, PAGES 2789-2792, AUGUST 1, 1998

Ultrafine aerosol particles in aircraft plumes: In situ observations

F.P. Schröder, B. Kärcher, A. Petzold, R. Baumann, R. Busen, C. Hoell, and U. Schumann

DLR Oberpfaffenhofen, Institut für Physik der Atmosphäre, Wessling, Germany

Abstract. Measurements of ultrafine particles in the near field of the DLR research aircraft ATTAS using low (0.02 g/kg fuel) and high (2.7 g/kg) fuel sulfur contents (FSCs) are presented. Soot emissions of $\sim 10^{15}$/kg show no significant dependence on FSC. Strong evidence is found that $\sim 1/3$ of the soot particles must be involved in ice nucleation in contrails, in addition to freezing of newly formed volatile particles. In the absence of contrails, numbers of volatile particles with diameters $D > 5$ nm reach $\sim 10^{17}$/kg for high FSC, and still reach $\sim 10^{16}$/kg for low FSC. A clear contribution of H_2SO_4 to volatile particle growth is observed. If growth is exclusively linked to H_2SO_4, the S to H_2SO_4 conversion efficiency increases with decreasing FSC. Depletion of ultrafine particles is observed in contrails, very likely due to scavenging by contrail ice crystals.

Introduction

Particles emitted by aircraft jet engines and formed *in situ* in young exhaust plumes can potentially induce the formation of new ice clouds (contrails), modify the microphysical properties of existing cirrus clouds, and provide sites for heterogeneous chemical reactions [*Friedl*, 1997; *Brasseur et al.*, 1998]. The impact of aircraft-produced aerosols upon chemistry and climate has recently received considerable attention. Characterization of particle size distribution and composition is one key step in assessing this impact.

Previous aerosol measurements in young jet plumes focused on contrail ice particles and condensation nuclei (CN) and the dependence of their properties on fuel sulfur content (FSC) [*Schumann et al.*, 1996; *Petzold et al.*, 1997]. Very recent measurements of ultrafine particles behind subsonic aircraft have been reported by *Anderson et al.* [1998]. The observations of particles with $D > 5$ nm (number per kg fuel, N_5) and with $D > 14$ nm (N_{14}) at plume ages $t = 0.5 - 20$ s (distances $100 - 3000$ m) presented in this work have been made during the SULFUR 5 field mission in April 1997, using the ATTAS as the source aircraft [*Busen et al.*, 1997]. Measurements were performed with two FSCs (low, or L and high, or H) and at two altitudes (background pressure 357 hPa, temperature $T = 231$ K, and relative humidity RH = 46%, no contrail formation, dry case D; 287 hPa, 219 K, 33%, contrail formation, wet case W).

Paper number 98GL02078.
0094-8534/98/98GL-02078$05.00

A few theoretical studies of plume microphysics have been published to date [*Kärcher*, 1996; *Brown et al.*, 1996; *Yu and Turco*, 1997]. In the companion paper [*Kärcher et al.*, 1998a] and in *Yu et al.* [1998], the data discussed here are further analyzed and compared with new model results.

Experiment and Data Evaluation

During SULFUR 5 ATTAS exhaust particles have been measured in the diameter range between about 5 nm and 20 μm. In Figure 1 we describe the CN counters (CNCs) together with the major components of the sampling payload. This new instrumentation enabled us to measure *in situ* CN number concentrations (symbol n) exceeding 10^6 cm^{-3}, and to distinguish between volatile and non-volatile components by exposing the sample to temperatures of about 500 K. Calibration of the CNCs yielded an uncertainty estimate ± 1 nm for the lower cut-off diameters. All other parts of the instrumentation to measure meteorological and turbulence parameters, as well as accumulation- and coarse mode particles by optical spectrometers (PCASP-100X for the size range $0.1 - 3$ μm; FSSP-300 for $0.3 - 20$ μm) are sim-

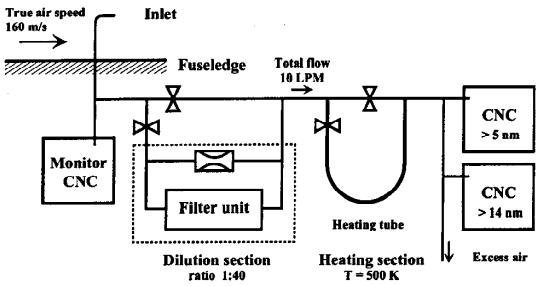

Figure 1. CN sampling payload aboard the FALCON with the backward-oriented, interstitial inlet (cut-off diameter ~ 1 μm). The sample flow was directed towards CNCs (modified TSI 3010 and 3760A [*Schröder and Ström*, 1997; *Mertes et al.*, 1995], measured 50% cut-off diameters indicated). The aerosol passes a passive dilution section (ratio 40 ± 9, 20% standard deviation) and/or a 1.5 m long heating section. To evaluate the data, a common coincidence correction was applied [*TSI*, 1996]. Overall diffusion losses for unheated $D = 5\,(14)$ nm particles under flight conditions are 15% (4%) [*Hinds*, 1982]. Data were not corrected for these losses.

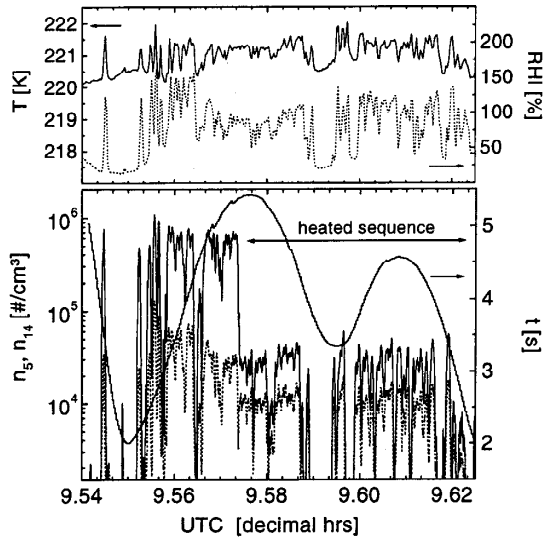

Figure 2. Representative time series of plume temperature, relative humidity over ice, CN number densities, and plume age vs universal time in the ATTAS contrail (case HW). The time series extends over 10 min, covering plume crossings at plume ages (distances) of ~ 2–5 s (300 – 800 m). During heating of particles in the CNCs (see arrow), significantly less particles with $D > 5$ nm (solid line) are detected, while larger (> 14 nm) particles (dashed line) are less affected.

ilar to previous SULFUR experiments [*Schumann et al.*, 1996; *Petzold et al.*, 1997].

In Figure 2 we present a typical time series containing T, relative humidity with respect to ice (RHI), n_5 and n_{14}, and t in a visible contrail 300 – 800 m behind the ATTAS for high FSC (case HW), as a function of the universal time UTC. Particle abundances have been acquired with 10 Hz temporal resolution, or about 20 m distance in the flight direction. Figure 2 displays the variability of the measured data. During contrail penetrations, n_5 rises to values above 10^6 cm^{-3}, four orders of magnitude greater than background concentrations. When the heating section is activated (see arrow), maximum n_5 values decrease by more than an order of magnitude, while n_{14} values are less affected. We note that RHI scatters around 100%, indicating the presence of ice particles, as expected from contrail simulations.

In order to facilitate the discussion of aerosol microphysics, we use the number N of particles per unit mass of fuel consumed instead of the measured n values. This quantity does not depend on plume dilution, and any observed changes of N with t directly reflect processes like particle growth due to condensation or coagulation. The overall dilution $\mathcal{D}$ of the expanding ATTAS wake is well-known from analyses of T and CO_2 data measured during SULFUR 5, video analyses of the plume cross-section development [*Petzold et al.*, 1998], and fluid-dynamical calculations [*Kärcher et al.*, 1998b]. Within their uncertainties, these independent methods yield $\mathcal{D} = (0.005/t\,[\mathrm{s}])^{0.9}$, valid for 5 ms < t < 20 s. Following *Schumann et al.* [1998], we employ $N = \lambda/\rho \cdot n/\mathcal{D}$, where λ is the air/fuel ratio at the engine's exit plane and ρ is the local mass density of air. The total uncertainty of N is mainly determined by the accuracy of the internal CNC dilution (Figure 1).

After removing all out-of-plume events, the data were sorted with respect to increasing plume age and grouped together in t intervals containing 300 single measurements each. From these statistical groups, we present the 95-percentile values (using the same symbol N, for simplicity), which in almost all cases cover the maxima and 90-percentiles within the 20% uncertainty of the single measurement. This evaluation strategy ensures that we mainly consider measurements related to full plume penetrations and that data taken apart from the plume center do not affect the results. Further, we reduce the effects resulting from fluctuations of the CNC dilution, since a single t interval does not necessarily represent data exclusively measured at a certain time.

Results and Discussion

Non-volatile aerosol. Figure 3 shows non-volatile particle abundances N_{14} derived for the cases LD (triangles), HD (squares), LW (circles), and HW (diamonds), with estimated error bars for LD and LW data. Since volatile components have been removed in the heating section, these data represent the emitted soot particles, N_s. At the flight level where no contrail formed (HD, LD), we find approximately constant values $N_s \simeq 1.7 \times 10^{15}$/kg for $t = 0.6 - 8$ s, despite the large variation of FSC. This confirms previously measured values of $1.6 \pm 0.2 \times 10^{15}$/kg (or ~ 0.1 g soot per kg fuel) for the ATTAS [*Petzold and Schröder*, 1998], and is consistent with the findings that the mean diameter

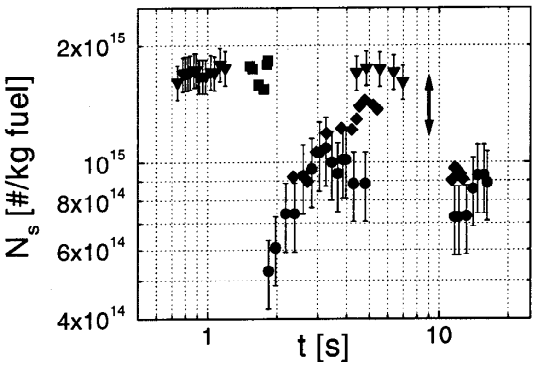

Figure 3. Soot particle abundances vs plume age behind the ATTAS. Shown are concentrations of particles with $D > 14$ nm that passed the heating section of the CNC (no contrail: squares HD, triangles LD; contrail: circles LW, diamonds HW). Soot emissions are independent of the fuel S level (cp. LD and HD). Approximately 1/3 of the emitted soot particles must have been involved in heterogeneous ice nucleation (see arrow between the D and W cases). For details, see text.

of the soot mode is 45 nm and that > 95% of all soot particles are larger than 14 nm [*Petzold et al.*, 1998].

Measurements inside contrails (HW, LW) yield ~ 15 – 40% lower peak values (HW: 1.4×10^{15}/kg; LW: 1.1×10^{15}/kg) and exhibit increasing trends between $t = 2 - 5$ s. (Data for $t < 2$ s are not available in these cases since encounters at distances < 300 m to the ATTAS were avoided for safety reasons.) The 'missing' soot fractions (HW: 3×10^{14}/kg; LW: 6×10^{14}/kg) are very likely incorporated into the contrail ice crystal mode. The following arguments support this conjecture. (1) The FSSP-300 observations, those made during SULFUR 4 [*Petzold et al.*, 1997], and related model simulations [*Kärcher et al.*, 1998b] show that the ice mode peaks at $D_{ice} \simeq 1.1\,\mu$m (H) and $1.3\,\mu$m (L). The interstitial aerosol inlet of the CNC does not allow the detection of particles with $D_{max} > 1\,\mu$m [*Schröder and Ström*, 1997]. Thus, part of the ice particles frozen onto soot cores were not counted. (2) The increasing trends in the LW and HW cases are very likely caused by evaporating, small ice crystals in the non-persistent contrail, because the crystals become accessible by the interstitial aerosol inlet while shrinking. The fact that the HW peak slightly exceeds the LW peak may be explained by the different values of $(D_{ice} - D_{max})$ in both cases. (3) The observations do not permit the derivation of a significant difference in the number of soot particles transformed into ice between L and H cases. However, they strongly suggest that ~ 18 – 35% of the emitted soot particles (see arrow in Figure 3) must have participated in ice nucleation.

This interpretation is supported by our simulation results, which further indicate that for high FSC a total number of 1.6×10^{15}/kg ice particles nucleate in the contrail (10^5 cm^{-3} at $t = 1$ s), that ~ 1/2 of them stem from homogeneous freezing of plume aerosols, and that, in relative terms, less particles freeze heterogeneously in the contrail with increasing FSC [*Kärcher et al.*, 1998b].

The N_s data attain a nearly constant level in case LW after $t = 3 - 4$ s, indicating that coagulation scavenging of soot by ice is unimportant on this timescale (see discussion below), although it may be efficient later in persistent contrails [*Ström and Ohlsson*, 1998]. A nearly constant value for N_s, albeit likely, cannot be derived from the data available in case HW. The measurements for $t > 10$ s took place 10 – 20 min (or ~ 100 km distance) later than those at earlier plume ages, and intermediate data are not available. Hence, both data sets may have been taken at different background conditions and are not directly comparable.

Volatile aerosol. Figure 4 shows unheated particle abundances $N(t)$, comprising N_5 (open symbols) and N_{14} data (filled symbols) for the L (triangles) and H cases (circles) without (Figure 4a) and with (Figure 4b) contrail. Since most soot particles are larger than 14 nm and particles in excess of $N_s \simeq 1.7 \pm 0.3 \times 10^{15}$/kg were removed by heating, the N values mainly represent volatile plume particles except for N_{14} low-S data (filled triangles).

The N_5 values for high FSC in Figure 4a (open circles) stay at a constant level of $1.2 - 1.5 \times 10^{17}$/kg, indicating that all detectable particles have grown past the CNC cut-off already at $t = 1$ s. In contrast, N_{14} increases (filled circles, fitted line), but stays more than a factor 10 below N_5. Hence, the mean diameter D of the observable ultrafine particle size distribution peaks within 5 – 14 nm. (The measurements do not exclude the presence of additional particles at sizes < 5 nm.) The N_5 values for low FSC (open triangles, fitted line) increase to $\sim 2 \times 10^{16}$/kg up to $t = 5$ s, while the corresponding N_{14} values (filled triangles) show no significant trend. This implies a smaller mean size $D < 5$ nm and a slower growth rate as compared to case HD, proving that oxidized sulfur in the form of H_2SO_4 participates in particle growth. (It cannot be ruled out that species other than H_2SO_4 did additionally condense on the particles.)

The observed trend of $N_5(t)$ in case LD is used to infer an overall growth rate, $R = dD/dt \simeq (D - D_0)/t$, of particles surpassing 5 nm, using the initial diameter $D_0 = 0.6$ nm of the molecular clusters. Because $D < 5$ nm for $t < 5$ s in case LD, we estimate $R_L = 0.48$ nm/s, with $D = 3$ nm and $t = 5$ s. Since $D > 5$ nm (but < 14 nm) already at $t = 1$ s in case HD, R_H must be larger. Using $D = 10$ nm and $t = 1$ s yields $R_H = 9.4$ nm/s, i.e., $R_H/R_L \simeq 20$, which is markedly less than the 150-fold increase of FSC between the L and H case. Under the premise that growth is solely linked to H_2SO_4 ($R \propto \eta$FSC, the radial growth rate does not depend on the particle size in the free molecular regime), this suggests different conversion efficiencies η of S to H_2SO_4 for the two FSCs, and that η increases by $\eta_L/\eta_H =$

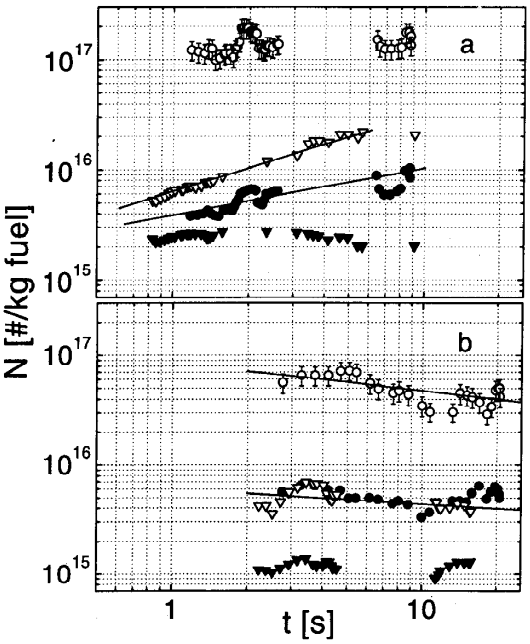

Figure 4. Total (mostly volatile) particle abundances vs plume age for case D (no contrail, 4a) and W (contrail formed, 4b). Shown are N_5 (open symbols) and N_{14} (filled symbols) for the L (triangles) and H cases (circles). Lines indicate S-induced particle growth (trends fitted to the data in 4a) and particle scavenging by contrail ice crystals (calculated trends in 4b, see text).

Pergamon

Atmospheric Environment Vol. 32, No. 18, pp. 3073–3077, 1998

Printed in Great Britain

PII: S1352–2310(97)00400–7

1352–2310/98 $19.00 + 0.00

JET ENGINE EXHAUST CHEMIION MEASUREMENTS: IMPLICATIONS FOR GASEOUS SO_3 AND H_2SO_4

F. ARNOLD,*,† TH. STILP,† R. BUSEN,‡ and U. SCHUMANN‡

†Max-Planck-Institut für Kernphysik, Atmospheric Physics Division, P.O. Box 10 39 80, D-69029 Heidelberg, Germany; and ‡Institut für Physik der Atmosphäre, DLR Oberpfaffenhofen, D-82230 Wessling, Germany

(*First received* 1 *May* 1997 *and in final form* 27 *August* 1997. *Published July* 1998)

Abstract—We have made mass spectrometric measurements of negative chemiions (CI) in the exhaust of a jet engine on the ground. The measurements took place at plume ages between 6.6 and 19 ms at low- and high-fuel sulfur content (FSC). Total negative CI-number densities reached up to $1.4 \cdot 10^7\ cm^{-3}$ corresponding to an emission index for negative CI of 3×10^{15} CI per kg fuel. The most abundant negative CI species were found to be $HSO_4^- H_2SO_4$, $HSO_4^- SO_3$, $HSO_4^- HNO_3$, and $NO_3^- (HNO_3)_m$. Probably HSO_4^--containing ions are formed from NO_3^--containing ions by reactions with SO_3 and gaseous sulfuric acid (GSA). Hence our experiments indicate the presence of SO_3 and GSA. Building on this ion reaction scheme the S(VI) number density (S(VI) = $SO_3 + H_2SO_4$) was inferred from the CI-composition measurements. For low FSC one obtains $(S(VI)) = 6.4 \times 10^{11}\ cm^{-3}$ which corresponds to an efficiency for fuel sulfur conversion to gaseous S(VI) of $\varepsilon = 0.012$. Our findings have important implications for bimolecular H_2SO_4–H_2O-nucleation in jet aircraft exhaust plumes at cruise altitudes. New aerosol particles may form via homogeneous and/or CI-induced nucleation while heterogeneous nucleation on soot particles may activate soot particles to become water vapour condensation nuclei. Our findings imply that nucleation and condensational growth are more efficient than predicted by most previous models which assumed smaller ε.

Key word index: Jet exhaust ions, S(VI).

INTRODUCTION

Jet engines are thought to produce gaseous sulfuric acid (GSA) by oxidation of fuel sulfur to SO_3 and subsequent SO_3-conversion to GSA. This is indicated by recent experiments (*cf.* Reiner and Arnold, 1993; Frenzel and Arnold, 1994). Since GSA is a very efficient aerosol forming gas it may produce aerosol particles in jet aircraft exhaust plumes. GSA may undergo with H_2O bi-molecular nucleation and condensation leading to new particles (by homogeneous nucleation (HONU) and ion-induced nucleation (INU)) and to coated soot particles by heterogeneous nucleation (HENU) (*cf.* Hofmann and Rosen, 1978; Reiner and Arnold, 1993; Miake-Lye *et al.*, 1994; Kärcher *et al.*, 1995; Zhao and Turco, 1995; Brown *et al.*, 1996b). H_2SO_4–H_2O-nucleation may influence water contrail formation and thereby eventually even cirrus cloud formation.

Most critical parameters controlling H_2SO_4–H_2O-nucleation are the efficiency ε of fuel sulfur conversion to S(VI) ($= SO_3 + H_2SO_4$), the efficiency of SO_3-conversion to GSA in the very early exhaust plume, and plume dilution.

Previous laboratory experiments have revealed that CI formed in jet fuel combustion are sensitively influenced by GSA and that therefore these CI may serve as tracers for GSA-detection in the jet fuel combustion (Frenzel and Arnold, 1994). Recently, the first mass spectrometric measurements in the exhaust of modern large turbofan engines at the ground have been reported by Arnold *et al.* (1997). These measurements which took place in a test channel and at a plume age $t_p = 0.1$ s revealed the presence of cluster ions with HSO_4^-- and NO_3^--cores similar to the results of the laboratory burner experiments of Frenzel and Arnold (1994). The test channel experiments indicate $\varepsilon = 0.015$ and an emission index for negative CI of $E \geqslant 2 \times 10^{15}$ CI per kg fuel consumed. The test channel measurements do not indicate the presence of the GSA-precursor SO_3 which suggests that SO_3-conversion to GSA is completed already at $t_p < 0.1$ s.

The present paper reports on mass spectrometric measurements of negative CI in the exhaust of a small jet engine at the ground at very small plume ages between 6.6 and 14 ms. Here for the first time SO_3 was detected. Evidently at the very small plume

*Author to whom correspondence should be addressed.